REFERENCES

[1] R. B. McGhee and A. Frank, "On the stability of quadruped creeping gait," *Math. Biosci.*, vol. 3, no. 314, pp. 331–351, Oct. 1968.

[2] A. Bessonov and A. Umnov, "The analysis of gaits in six-legged vehicle according to their static stability," in *Proc. Symp. Theory Practice Robots*, Udine, Italy, 1973, pp. 1–9.

[3] S. M. Song and B. S. Choi, "The optimally stable ranges of $2n$-legged wave gaits," *IEEE Trans. Syst., Man, Cybern.*, vol. 20, July/Aug. 1990.

[4] E. I. Kugushev and V. S. Jaroshevskij, "Problems of selecting a gait for an integrated locomotion robot," in *Proc. 4th Int. Conf. Artificial Intelligence*, Tbilisi, U.S.S.R., Sept. 1975, pp. 789–793.

[5] R. B. McGhee and G. I. Iswandhi, "Adaptive locomotion of a multilegged robot over rough terrain," *IEEE Trans. Syst., Man, Cybern.*, vol. SMC-9, Apr. 1979.

[6] F. Ozguner, S. I. Tsai, and R. B. McGhee, "An approach to the use of terrain-preview information in rough-terrain locomotion by a hexapod walking machine," *Int. J. Robot. Res.*, vol. 3, pp. 134–146, Summer 1984.

[7] S. Hirose, "A study of design and control of a quadruped walking vehicle," *Int. J. Robot. Res.*, vol. 3, pp. 113–133, Summer 1984.

[8] M. Jamshidi and P. J. Eicker, *Robotics and Remote Systems for Hazardous Environments*. Englewood Cliffs, NJ: Prentice-Hall, 1993.

[9] H. J. Chiel, R. D. Beer, R. D. Quinn, and K. S. Espenshied, "Robustness of a distributed neural network controller for locomotion in a hexapod robot," *IEEE Trans. Robot. Automat.*, vol. 8, pp. 293–303, June 1992.

[10] P. V. Nagy, S. Desa, and W. L. Whittaker, "Energy based stability measures for reliable locomotion of statically stable walkers: Theory and application," *Int. J. Robot. Res.*, vol. 13, no. 3, pp. 272–287, 1994.

[11] T. T. Lee, C. M. Liao, and T. K. Chen, "On the stability properties of hexapod tripod gait," *IEEE J. Robot. Automat.*, vol. 4, pp. 427–434, Aug. 1988.

Intelligent Compliant Motion Control

Omar M. Al-Jarrah and Yuan F. Zheng

***Abstract*—The role of a compliant motion scheme is to control a robot manipulator in contact with its environment. By accommodating with the interaction force, the manipulator can be used to accomplish tasks that involve constrained motions. This paper presents a new work on the compliant motion control for position-controlled manipulator. A new method for achieving efficient interaction between the manipulator and its environment is developed. The interaction force is reduced using a quadratic cost function. In this method, the compliance is formulated as function of the interaction force. An adaptive element is used to update the compliance. The stability of the system is investigated using the Lyapunov approach. Experiments are conducted in our laboratory to demonstrate the use of such scheme.**

I. INTRODUCTION

Many applications in the manufacturing and service industries require manipulators to make contact with environments [1]–[4]. For example, inserting a peg in a hole, turning a crank, grinding, polishing, teleoperating, and bending a flexible beam. Its common to all of those applications that the motion of the manipulator's end-effector is constrained by the environment. In recent years, two notable approaches dealing with this problem have been proposed. One approach uses a hybrid position/force control scheme to control the position in those directions where there is no constraint and to control the force in the constrained direction [5], [6]. The second approach realizes the fact that the end-effector must comply with the interaction force. Otherwise, rejecting the interaction force will result in instability and possibly damage to either the end-effector or the environment or both. This can be done using a compliant motion control scheme [7].

Compliance can be either passive or active. Passive compliance is achieved by attaching a spring-damper device to the end-effector. Remote center compliance (RCC) is an example of passive compliance which is used for the peg-in-a hole problem [8]. Passive devices such as RCC are task-oriented devices and places extra loading on the end-effector. On the other hand, active compliance uses a compliant motion control scheme which is not restricted to a specific task and places no loading on the end-effector.

The core of the active compliant motion is the concept of mechanical impedance in which both the dynamic behavior and the position of the manipulator are controlled [9]. Several adaptive compliant and impedance motion control schemes were devised [7], [10]–[13]. It is common for those schemes to use combinations of proportional, integral, and derivative controls plus nonlinear compensation for the gravity, centrifugal, and coriolis terms in the manipulator dynamics.

Compliant motion introduces a force feedback loop which affects the stability of the system. Stability analysis of several compliant control schemes has been addressed by several researchers. The stability of the system depends on the desired impedance parameters. The impedance of the environment greatly affects the stability analysis of the system.

In a position control system, compliant motion is similar to what is believed to take place in biological systems [14]. Control of human movement is believed to have a hierarchical structure of three levels. The highest level in the motor control hierarchy is in the association cortex in which needs are converted into motor plans that are relevant to the context. The middle level is the projection system in which motor plans are transformed into motor programs that control different aspects of motion. Motor programs are updated according to the tasks (learning). The spinal cord is the lowest level in the motor control hierarchy. It converts the motor commands into muscular activity which are regulated by the spinal cord using reflexes.

In this paper, a new compliant motion control scheme is proposed based on what is believed to take place in biological systems. In this scheme, the compliance of the manipulator is changed in accordance with the sensed force and varies in a way that speeds up the reduction of the interaction forces. To accomplish this, a quadratic cost function is defined on the interaction force and the compliance is updated in the steepest decent direction. The stability of the proposed scheme is investigated using the Lyapunov approach.

This paper is organized as follows. Intelligent compliant motion control is formulated in the next section. The third section is devoted for studying the stability of the system. Advantages and limitations of this approach are discussed in the fourth section, while the fifth section presents an application for this scheme. The experimental results are presented in the sixth section. Finally, the paper is concluded in the seventh section.

II. INTELLIGENT COMPLIANT MOTION CONTROL

We will consider the case where the compliance is provided for the robot using an external control loop as shown in Fig. 1. Consider

Manuscript received April 15, 1996; revised November 25, 1996. This work was supported by the National Science Foundation under Grant IRI-9405276.

The authors are with the Department of Electrical Engineering, The Ohio State University, Columbus, OH 43210 USA (e-mail: zheng@ee.eng.ohio-stat.edu).

Publisher Item Identifier S 1083-4419(98)00215-5.

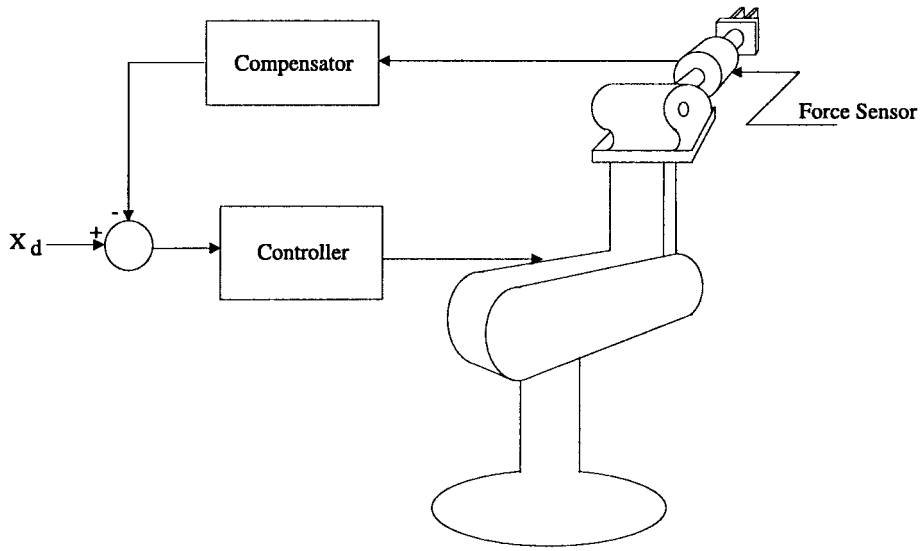

Fig. 1. Compliant motion control.

a position-controlled robot. Many other researchers [15]–[17], have used a set of linear decoupled equations to model the dynamics of the system. It should be noted that the modeling is not for a bare robot but the robot and its controller. The controller of the robot has already taken in consideration the nonlinear and coupling factors. As a result, the robot has become a position-controlled device in the Cartesian coordinates. The controller makes the motion of the robot not only linear but also decoupled in the Cartesian coordinates. Consequently, we can use a second order linear system to model the end-effector positioning system along each coordinate. That is, the end-effector position/orientation can be expressed as

$$x = \frac{w_0^2 x_d}{p^2 + 2\xi w_0 p + w_0^2} = G x_d \tag{1}$$

where x_d is the desired position/orientation, w_0 is the natural frequency, p is the differential operator, and ξ is the damping ratio.

In the modeling of the environment, we will assume that its dynamics is dominated by its stiffness. Thus, the interaction force F can be expressed as

$$F = K_e(x - x_e) \tag{2}$$

where K_e is the equivalent stiffness of the environment and the force sensor and x_e is the nominal position of the environment. We will assume that x_e is zero for simplicity of presentation.

Compliant motion controllers specify the relation between the force measured at the end-effector and the deviation from the desired trajectory. This can be achieved by using an external control loop which is sensitized by the force sensed by a wrist sensor (see Fig. 2). This compliant motion scheme is similar to a reflexive action in human beings. In this case the event that evokes this reflexive action is the sensed force while the reflexive action is to backup from the desired position. This can be formulated as

$$\delta x = HF \tag{3}$$

where δx is the deviation from the desired trajectory, H is a compensator that represents the compliance of the end-effector, and F is the force exerted on the end-effector. Mostly, it is desirable to have the end-effector behaving as a spring-damper, that is

$$H = \frac{1}{bp + k} \tag{4}$$

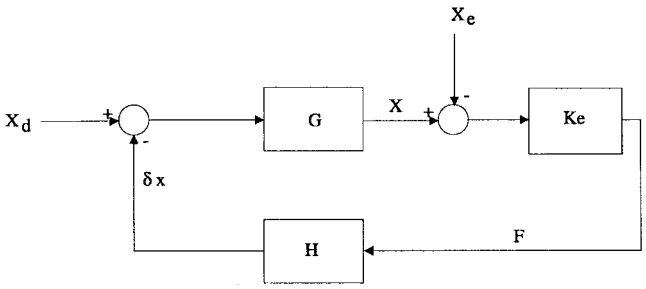

Fig. 2. Block diagram of compliant motion control.

where b is the damping of the damper and k is the stiffness of the spring. The quantity $\frac{1}{bp+k}$ is referred to as the compliance or mechanical admittance.

In conventional compliant motion control schemes, the parameters b and k in (4) are constants. Furthermore, the stiffness of the environment is assumed to be constant. However, there are many applications in which the stiffness of the environment is not constant. For example, consider the task of bending a flexible sheet. The stiffness of the sheet is a nonlinear function of the bending angle. Also, in those applications which involve a man–machine interaction, the stiffness of the environment is not constant and changes with the interaction force. On the other hand, adaptive compliant controller uses a time varying parameters that are updated either to ensure a stable behavior of the system or to match a reference model [7], [10]–[13]. Nonetheless, an intelligent compliant control scheme similar to that in human beings can be used to provide a mechanism for the manipulator to interact with a complicated environment. The stiffness of the arm varies with the load sensed by the force sensors. If the load on the arm is changed, the stiffness of the arm will change accordingly. This motivates us to do similar thing for the compliance in robotics.

We propose to update the compliance of the end-effector by imposing a gain on the original compliant motion compensator. This gain will be changed according to the nature of the interaction force. Therefore, the compliance of the end-effector will be updated accordingly.

The deviation from the desired trajectory δx can be redefined as

$$\delta x = HcF \tag{5}$$

where c is a gain to be used for controlling the compliance.

There are different criteria which can be used to update the gain c. One can associate with c a cost function that indicates the goodness of the change in c. By using the gradient algorithm, the gain can be updated in the direction that will minimize the cost function. We propose to use a quadratic cost function defined as

$$E = \frac{1}{2}F^2(c). \tag{6}$$

From (5), note that c directly affects the interaction force since any change in c will affect δx which in turn will affect F. Therefore, this cost function can be used to update the compliance.

By using the standard gradient algorithm, we obtain

$$\Delta c = -\upsilon \frac{dE}{dc} \tag{7}$$

where υ is a positive constant that defines the adaptation gain. From (6) we have

$$\frac{dE}{dc} = F\frac{\partial F}{\partial c}. \tag{8}$$

From Fig. 2, the end-effector position/orientation can be expressed as

$$x = \frac{Gx_d}{1 + GHK_e c}. \tag{9}$$

By substituting for x in (2), the interaction force can be expressed as

$$F = \frac{K_e G x_d}{1 + GHK_e c}. \tag{10}$$

From (10), we obtain

$$\frac{\partial F}{\partial c} = -K_e^2 G^2 H \frac{x_d}{(1 + GHK_e c)^2} \tag{11}$$

and

$$\frac{\partial F}{\partial K_e} = \frac{Gx_d}{(1 + GHK_e c)^2}. \tag{12}$$

One can see that changes in the force with respect to c oppose changes of the force with respect to K_e. Furthermore, we can express (11) in terms of (12) to obtain

$$\frac{\partial F}{\partial c} = -K_e^2 GH \frac{\partial F}{\partial K_e}. \tag{13}$$

Substituting (13) in (7), we obtain

$$\Delta c = \upsilon F K_e^2 GH \frac{\partial F}{\partial K_e}. \tag{14}$$

One can estimate the unknowns in (14) using the fact that K_e, G, and H are bounded transfer functions, i.e.,

$$K_e^2 GH \frac{\partial F}{\partial K_e} \leq \rho \frac{\partial F}{\partial K_e} \tag{15}$$

where ρ is some constant. From (15), we can simplify Δc in (14) to obtain

$$\Delta c = lF \frac{\partial F}{\partial K_e} \tag{16}$$

where l is some constant.

The adaptation law in (16) cannot be computed on line since $\frac{\partial F}{\partial K_e}$ is unknown. To estimate $\frac{\partial F}{\partial K_e}$, any change in the force is assumed to be a change in the stiffness. This assumption is very reasonable in the context of compliant motion. From (2) and (10), one can see that the manipulator can only detect changes in the sensed force. Changes in the reference trajectory or in the desired force will result in changes in the sensed force. Those changes in the force are always interpreted as changes in the stiffness of the environment. To explain that, we will consider the factors that may result in a change in the sensed force. These factors are the stiffness of the environment, the desired or reference trajectory, and the desired force. Therefore, an estimate of $\frac{\partial F}{\partial K_e}$ would be the change in the interaction force. Substituting for $\frac{\partial F}{\partial K_e}$, we obtain

$$\Delta c = l(F[t] - F[t - \Delta t])F[t] \tag{17}$$

where Δt is the sampling period. Thus, the compliance parameter c is modified such that

$$c[t + \Delta t] = c[t] + l(F[t] - F[t - \Delta t])F[t]. \tag{18}$$

One can see that the compliance changes according to the change in the force. As a matter of fact, (18) indicates two important features of the intelligent compliant motion control. First, the change in the compliance gain is proportional to the change in the interaction force. If the interaction force changes, the compliance will increase or decrease accordingly. Secondly, this change is proportional to the interaction force itself, which means that the change in the force is scaled by the amount of the interaction force.

The computational cost of the intelligent compliant motion control can be studied by considering a digital equivalent of the system. Consider a first order difference approximation of the differential operator. The intelligent compliant motion control can be written as

$$\delta x[t + \Delta t] = \phi \delta x[t] + \gamma F[t] c[t + \Delta t] \tag{19}$$

where $\phi = (1 - \frac{k\Delta t}{b})$ and $\gamma = \frac{\Delta t}{b}$.

Thus, this new algorithm requires two steps. In the first step, the compliance gain c is updated according to (18). Then, in the second step, the deviation from the reference trajectory is calculated according to (19). Therefore, four multiplications and three additions/subtractions are involved in this scheme.

III. Stability Analysis

Because of the limited space, the stability analysis is conducted based on the simplified model of the robotic system, a set of second order linear systems as defined in (1). From (1), the trajectory of the end-effector is given by

$$\ddot{x} + 2\xi w_0 \dot{x} + w_0^2 x = -w_0^2 \delta x. \tag{20}$$

From (5), the deviation from the desired trajectory δx is given by

$$b\delta\dot{x} + k\delta x = cK_e x. \tag{21}$$

The trajectory of the compliance's gain c in (17) can be expressed in the continuous time as

$$\dot{c} = l\dot{F}F. \tag{22}$$

However, from (2), one can obtain

$$\dot{c} = lK_e(K_e\dot{x} + \dot{K}_e x)x. \tag{23}$$

We will use the Lyapunov approach to study the stability of the system [18], [19]. Consider the following candidate Lyapunov function:

$$v(\dot{x}, x, \delta x, c) = \frac{\dot{x}^2}{2w_0^2} + \frac{1}{2}(x - \delta x)^2 + \frac{\xi}{4w_0}c^2. \tag{24}$$

This is a positive semidefinite function. A sufficient condition for the stability of the system is that the derivative of v along the trajectories of the system in (20), (21), and (23) to be negative.

By taking the derivative of (24) along with (20), (21), and (23), one can obtain

$$\dot{v}(\dot{x}, x, \delta x, c) = [\dot{x} \quad x \quad \delta x]\, P \begin{bmatrix} \dot{x} \\ x \\ \delta x \end{bmatrix} \tag{25}$$

where P is given by

$$P = \begin{bmatrix} -\frac{2\xi}{w_0} & \frac{lcK_e^2\xi}{4w_0} & -1 \\ \frac{lcK_e^2\xi}{4w_0} & -\frac{cK_e}{b} + \frac{lcK_e\dot{K}_e\xi}{2w_0} & \frac{k+cK_e}{2b} \\ -1 & \frac{k+cK_e}{2b} & -\frac{k}{b} \end{bmatrix}. \tag{26}$$

Note that $\dot{v}$ in (25) is a quadratic function. Therefore, it is negative semidefinite if and only if P is negative semidefinite. In order for P to be negative semidefinite, the following conditions must be satisfied:

$$32\frac{\xi}{w_0}\left(\frac{lcK_e\dot{K}_e\xi}{2w_0} - \frac{cK_e}{b}\right) + \frac{l^2c^2K_e^4\xi^2}{w_0^2} \le 0 \tag{27}$$

$$\frac{k}{b}\left(\frac{lcK_e\dot{K}_e\xi}{2w_0} - \frac{cK_e}{b}\right) + \frac{(cK_e+k)^2}{4b^2} \le 0 \tag{28}$$

$$\begin{aligned} &16ckK_e\xi(w_0 - lK_eb\xi) - 8\xi w_0\left(k^2 + c^2K_e^2\right) - l^2c^2K_e^4\xi^2bk \\ &\quad + 4lcK_e^2\xi w_0bk + 4lc^2K_e^3\xi w_0b + 8lcK_e\dot{K}_ew_0\xi b^2 \\ &\quad - 16cK_ew_0^2b \le 0 \end{aligned} \tag{29}$$

and

$$\frac{k}{b} \ge 0. \tag{30}$$

The most critical conditions are those given in (27) and (28). These inequalities show the dependency of the stability of the system on the stiffness of the environment and its rate of variation. As a matter of fact (27) and (28) show that the system will become unstable if we use a high adaptation gain. Furthermore, the sign of the adaptation gain l should oppose the sign of the rate of variation in the stiffness of the environment. Therefore, if the environment becomes stiffer, the stiffness of the end-effector should be reduced to improve the stability of the system.

IV. Application

In this section, we will address the bending of a flexible sheet as a possible application of the proposed scheme.

Zheng and Chen [20] proposed the use of minimization of forces and moments exerted on the end-effectors as a criterion of the trajectory planning. They studied the trajectory planning of two manipulators to deform a flexible beam. Optimal motion trajectories were derived to generate zero interaction moments. While the beam is being deformed, forces and moments should be applied to the beam. For example, in the manufacturing of printed wiring boards (PWB) (Fig. 3), a book is formed from a large number of elastic sheets and laminated to form a PWB. Some of the sheets are covered with electronic circuits and should be carefully aligned. For the alignment purpose, each sheet is equipped with four holes that should be aligned with four alignment pins on the assembly bed. It is difficult to align the four holes simultaneously because of the small tolerance between the pins and the holes. Thus, the manipulators should bend the sheet to align the middle holes with the corresponding pins. Then, they unfold the sheet to align the rest of the holes. However, the optimal trajectory are complicated and not suitable for real time application. A piece-wise linear approximation can be used to approximate the optimal trajectories [4].

Trajectories which are based on the optimal bending model are open loop trajectories without any feedback from the environment [20]. It is found that both position and orientation of the end effectors need to follow the optimal trajectory in which the two end points of the beam coincide with its zero moment (ZM) points and the deflection angle of the beam and the orientation of the two end-effectors are the same [20]. Under these conditions, the end-effectors are exposed to minimum forces and zero moments since the end-effectors are holding the ZM points. The force is given by

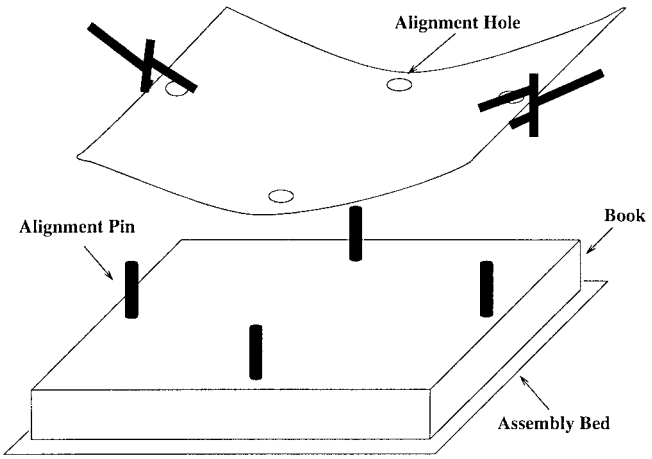

Fig. 3. Two end-effectors aligning a flexible sheet to form a PWB.

$$F = \frac{(2R(\alpha))^2 EI_z}{L^2} \tag{31}$$

where E is the stiffness of the beam, I_z is the moment of inertia of the beam cross section, L is the length of the beam, α is the bending angle of the beam, and $R(\alpha)$ is calculated from an elliptic integral [20].

The optimal trajectories are functions of the orientation of the end-effectors α, and should satisfy

$$x = L\left(\frac{P(\alpha)}{R(\alpha)} - \frac{1}{2}\right) \tag{32}$$

and

$$y = \frac{L}{R(\alpha)}\sin\left(\frac{\alpha}{2}\right) \tag{33}$$

where $P(\alpha)$ is calculated from another elliptic integral [20].

By using piece-wise linear approximation, the target bending angle α is divided into a number of smaller angles. The optimal trajectories are approximated by linear functions during the motion between any set of two consecutive points [4].

From (31), one can see the nonlinearity of the bending force as a function of the bending angle. Furthermore, under the piece-wise linear approximation of the optimal trajectories, the bending moment is no longer zero. It guarantees minimum forces and moments only at the end points of each piece. In the middle of the linear pieces, both forces and moments can be very high. Furthermore, for a small bending angle, approximation errors will drive the system to the case where the two end-effectors are pushing toward each other without any significant change in the orientation [4]. Therefore, due to the approximation errors, the apparent stiffness of the sheet will be very large for small bending angles.

Consider the use of a compliant motion control scheme for reducing the bending moment which results form the approximation errors. Because of the sensitivity of the bending process to approximation errors for small bending angles, the sheet will appear to be very stiff. Therefore, a small compliance should be used. Otherwise, approximation errors will be over compensated and the bending moment could be very large which will result in instability. However,

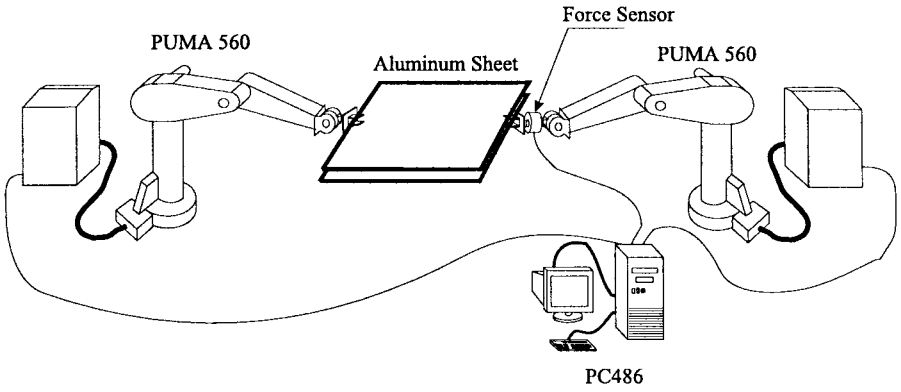

Fig. 4. Experimental setup.

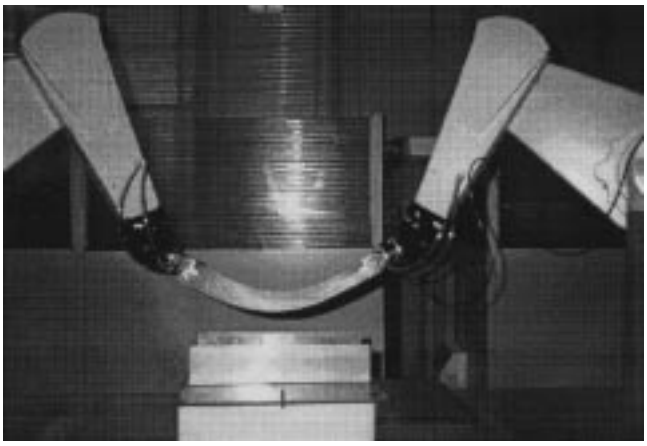

Fig. 5. Two PUMA robots bending aluminum sheets.

as the bending angle increased, larger compensation are required to reduce the bending moment. Thus, large compliance should be used. In the case of the conventional compliant motion control, the compliance is constant. On the other hand, using the intelligent compliant motion control, one can use a small compliance at the beginning of motion and the compliance will increase if the bending moment increased. Therefore, we can achieve high reduction of the bending moment for small and large bending angles.

V. Experimental Study

We have conducted experiments to demonstrate and verify the proposed schemes. In our experiments, we used two PUMA 560 robots to bend two aluminum sheets (Fig. 4). Each robot held one end of the sheet. One of the robots was equipped with a multi-axis force/torque sensor (intelligent multiaxis force/torque sensor system). The sensor was connected to a local controller that calculated the force/torque components from the raw data and provided a temperature compensation and a filter [21]. The supervisor computer communicated with the sensor controller via a serial port.

The PUMA robot was positionally controlled with each joint having its own controller. The joint controller received a command every 28 ms. Thus, we could send a position command to the joint controllers every 28 ms (ALTER mode in the VAL II language) [22].

The experiments (Fig. 5) resembled the production of the PWB example as mentioned in the previous section. In the experiments the robots had to move to a pre-specified position and to pick up the aluminum sheet. After that, the robots moved to another specified position where the bending process occurred. The sheet was bent to

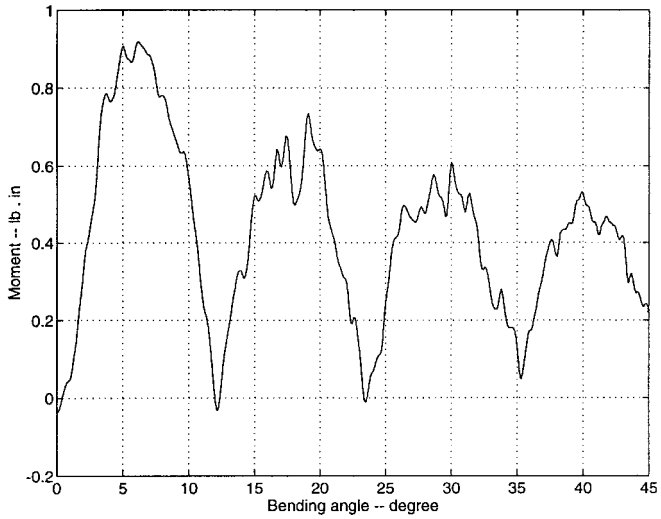

Fig. 6. Moment without compliant motion control.

make the two middle holes aligned with pins first. Finally, the robots extended the sheet to align the rest of the holes. The data from the force sensor was very noisy. This was due to the vibration of the end-effector during the robot motion. To get rid of the noise a low pass filter (LPF) with cutoff frequency of 10 Hz was added.

The bending moment was used as a criterion for the performance of the bending process [4]. The reason for that was that in the optimal case, the robot only provided a bending force and the bending moment was zero [20]. As mentioned in the previous section, due to the complexity of the optimal trajectories, a piece wise linear approximation was used. In this method, the optimal trajectories were calculated off line only at the end of every linear piece. The target bending angle was selected to be $\frac{\pi}{4}$.

We first ran the system without compliant control. Fig. 6 shows the results when the linear piece is a 0.2 rad interval. One can see that the bending moment is peaked between the two endpoints of every linear piece and is zero at the ends of the pieces. Furthermore, it is clear from Fig. 6 that the stiffness of the sheet is nonlinear function of the bending force and moment.

To prove the advantage of the proposed scheme, both the conventional and the intelligent compliant motion control schemes were used to bend the sheets. In the conventional case, the parameters of the compliant controller were selected to be

$$B = \begin{bmatrix} 0.56 & 0 \\ 0 & 0.025 \end{bmatrix} \tag{34}$$

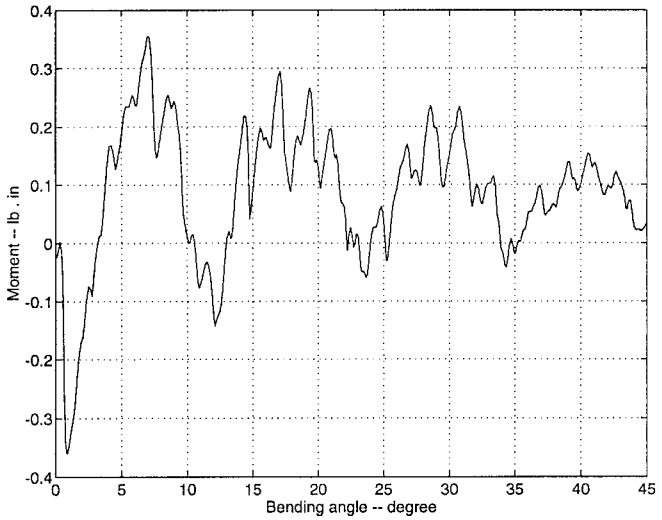

Fig. 7. Moment with conventional compliant motion control.

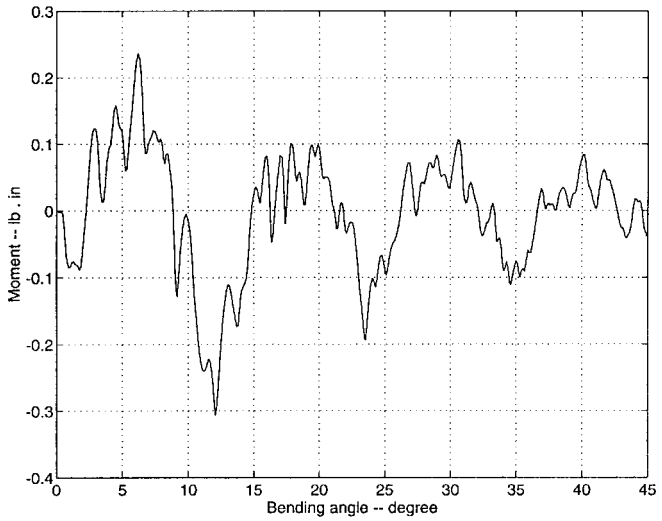

Fig. 8. Moment under intelligent compliant motion control.

and

$$K = \begin{bmatrix} 18 & 0 \\ 0 & 0.78 \end{bmatrix}. \tag{35}$$

The gain c was selected to be unity for both directions. The result of this experiment is shown in Fig. 7. One can see that the bending moment increased at the beginning of the bending process due to the over compensation. In addition, the reduction of the bending moment is not significant for large bending angles. If the gain is reduced, the moment will be reduced at the beginning and it will be large for larger angles.

In the case of the intelligent compliant motion control scheme the stiffness and damping parameters were selected to be similar to that in (34) and (35). The adaptation rate was selected to be

$$l = \begin{bmatrix} 0.1 & 0 \\ 0 & 0.5 \end{bmatrix}. \tag{36}$$

The gain c was initialized to

$$c = \begin{bmatrix} 0.5 & 0 \\ 0 & 0.8 \end{bmatrix}. \tag{37}$$

The bending moment is shown in Fig. 8, while the gains in the moment and force directions are shown in Figs. 9 and 10, respectively. It is clear from Fig. 8 that the performance of the

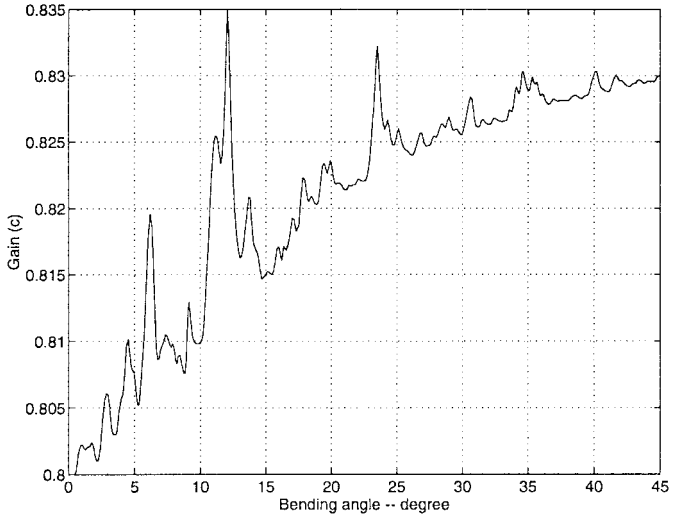

Fig. 9. Moment compliance gain c under intelligent compliant motion control.

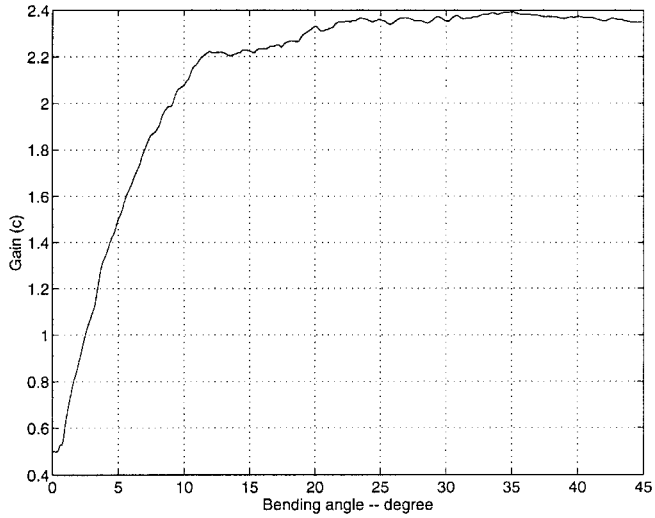

Fig. 10. Force compliance gain c under intelligent compliant motion control.

proposed scheme is better than that of the conventional compliant motion scheme because the bending moment is substantially less than the one shown in Fig. 6. Furthermore, the gains on the moment and the force in Figs. 9 and 10 increased with the increase of the moment and the force, respectively. Following the discussion in the previous section, the gains were initialized to small values to accommodate with small approximation errors. After that, both of the gains started to behave according to the bending moment and force. When the bending moment became small, both of the gains were saturated to steady state values. It can be noted that the gains became larger for larger values of the moment and the force and therefore, a larger reduction in the moment was obtained compared to the conventional compliant motion scheme. In addition, the negative peak of the bending moment at the beginning of motion was reduced significantly because the gains were initially small.

VI. Conclusion

Conventional compliant motion control uses a constant compliance. In reality, however, the impedance of the environment may vary. As a result, constant compliance renders undesired performance of a robot manipulator which interacts with the environment. In this paper, we

have proposed a new compliant motion control scheme. The proposed scheme was designed to vary the robot compliance in accordance with its interaction force with the environment. The purpose is to reduce the interaction force quicker such that the robot comply with the environment better. We have used the gradient method to update the compliance of the manipulator. To update the compliance, a gain was imposed on the interaction force and modified accordingly. This method has superiority over the conventional compliant motion in those applications in which the stiffness of the environment is not constant. The stability of the system using the new compliant scheme was investigated using the Lyapunov approach.

The new compliant scheme was verified by an application, namely, bending of a flexible sheet. The experimental results presented in the previous section prove that the mechanism developed in this paper is better than conventional compliant approaches for those applications in which the stiffness of the environment is not constant.

REFERENCES

[1] H. Kazerooni, T. B. Sheridan, and P. K. Houpt, "Robust compliant motion for manipulators, part I–II," *IEEE J. Robot. Automat.*, vol. RA-2, no. 2, pp. 83–105, 1986.

[2] J. M. Tao, J. Y. S. Luh, and Y. F. Zheng, "Compliant coordination control of two moving industrial robots," *IEEE Trans. Robot. Automat.*, vol. 6, pp. 322–330, June 1990.

[3] P. S. Schenker, A. K. Bejczy, W. S. Kim, and S. Lee, "Advance man-machine interfaces and control architecture for dexterous teleoperations," in *IEEE Oceans'91*, "Underwater Robotics" session, Honolulu, HI, Oct. 1991.

[4] O. Al-Jarrah, Y. F. Zheng, and K. Yi, "Trajectory planning for two manipulators to deform flexible materials using compliant motion," in *Proc. 1995 IEEE Int. Conf. Robotics Automation*, Nagoya, Japan, May 1995, pp. 1517–1522.

[5] S. Hayati, "Hybrid position/force control of multi-arm cooperating robots," in *Proc. 1986 IEEE Int. Conf. Robotics Automation*, San Francisco, CA, Apr. 1986, pp. 82–89.

[6] T. Yoshikawa and X. Zheng, "Coordinated dynamic hybrid position/force control for multiple robot manipulators handling one constrained object," in *Proc. 1990 IEEE Int. Conf. Robotics Automation*, Cincinnati, OH, May 1990, pp. 1178–1183.

[7] R. Colbaugh and A. Engelmann, "Adaptive compliant motion control of manipulators: Theory and experiments," in *Proc. 1994 IEEE Int. Conf. Robotics Automation*, San Diego, CA, May 1994, pp. 2719–2726.

[8] H. Asada and Y. Kakumoto, "The dynamic RCC hand for high-speed assembly," in *Proc. 1988 IEEE Int. Conf. Robotics Automation*, Philadelphia, PA, Apr. 1988, pp. 120–125.

[9] N. Hogan, "Impedance control: An approach to manipulation, parts I–III," *ASME J. Dynam. Syst., Meas. Contr.*, vol. 107, pp. 1–24, 1985.

[10] G. Niemeyer and J. J. E. Slotine, "Computational algorithms for adaptive compliant motion," in *Proc. 1989 IEEE Int. Conf. Robotics Automation*, Scottsdale, AZ, May 1989, pp. 566–571.

[11] R. Kelly, R. Carelli, M. Amestegui, and R. Ortega, "On adaptive control of robot manipulators," in *Proc. 1989 IEEE Int. Conf. Robotics Automation*, Scottsdale, AZ, May 1989, pp. 572–577.

[12] S. K. Singh, "Adaptive control of manipulator interaction with environment: Theory and experiments," in *Proc. 1993 IEEE Int. Conf. Robotics Automation*, Atlanta, GA, May 1993, pp. 1001–1006.

[13] H. Seraji, "Adaptive admittance control: An approach to explicit force control in compliant motion," in *Proc. 1994 IEEE Int. Conf. Robotics Automation*, San Diego, CA, May 1994, pp. 219–224.

[14] V. Brooks, *The Neural Basis of Motor Control*. New York: Oxford Univ. Press, 1992.

[15] D. A. Lawrence, "Impedance control stability properties in common implementations," in *Proc. 1988 IEEE Int. Conf. Robotics Automation*, Philadelphia, PA, Apr. 1988, pp. 1185–1190.

[16] Y. Xu and R. P. Paul, "On position compensation and force control stability of a robot with compliant wrist," in *Proc. 1988 IEEE Int. Conf. Robotics Automation*, Philadelphia, PA, Apr. 1988, pp. 1173–1178.

[17] H. Kazerooni and T. I. Tsay, "Stability criteria for robot compliant maneuvers," in *Proc. 1988 IEEE Int. Conf. Robotics Automation*, Philadelphia, PA, Apr. 1988, pp. 1166–1172.

[18] H. K. Khalil, *Nonlinear Systems*. New York: Macmillan, 1992.

[19] M. Vidyasagar, *Nonlinear Systems Analysis*. Englewood Cliffs, NJ: Prentice-Hall, 1978.

[20] Y. F. Zheng and M. Z. Chen, "Trajectory planning for two manipulators to deform flexible beams," *Robot. Auton. Syst.*, vol. 12, pp. 55–67, 1994.

[21] *Intelligent Multi-Axis Force/Torque Sensor System Manual*, Assurance Technol., Inc., 1991.

[22] *Unimate Industrial Robot Programming Manual Users's Guide to VALII*, Westinghouse Co., 1986.